Predictive exoskeleton control for arm-motion augmentation based on probabilistic movement primitives combined with a flow controller

Marko Jamšek[1,2], Tjaša Kunavar[1,2], Urban Bobek[1], Elmar Rueckert[3] and Jan Babič[1]

Abstract—There are many work-related repetitive tasks where the application of exoskeletons could significantly reduce the physical effort by assisting the user in moving the arms towards the desired location in space. To make such control more user acceptable, the controller should be able to predict the motion of the user and act accordingly. This paper presents an exoskeleton control method that utilizes probabilistic movement primitives to generate predictions of user movements in real-time. These predictions are used in a flow controller, which represents a novel velocity-field-based exoskeleton control approach to provide assistance to the user in a predictive way. We evaluated our approach with a haptic robot, where a group of twelve participants had to perform movements towards different target locations in the frontal plane. We tested whether we could generalize the predictions for new and unknown target locations whilst providing assistance to the user without changing their kinematic parameters. The evaluation showed that we could accurately predict user movement intentions while at the same time significantly decrease the overall physical effort exerted by the participants to achieve the task.

Index Terms—Physical Human-Robot Interaction, Physically Assistive Devices, Prosthetics and Exoskeletons

I. INTRODUCTION

R OBOTIC exoskeletons are promising tools to assist humans in various real-life tasks [1]. They are designed to be worn on the body and to provide direct motion assistance to the user. The two common applications of exoskeletons are physical rehabilitation for impaired patients [2] and motion augmentation of able-bodied workers [3]. In physical rehabilitation, the exoskeleton is used to move the limbs of impaired individuals based on repetitive motion patterns defined by physiotherapists [4], while for able-bodied workers the exoskeleton rather amplifies the user's joint torques [5]. Popular control approaches for these exoskeletons are

usually position or angle based for rehabilitation purposes or impedance/admittance based for movement augmentation [6], [7]. However, such control approaches lack the intention recognition needed for a successful human-robot interaction [8]. Since movement intention and prediction is a very complex problem, it is usually addressed by monitoring muscle or brain activity. Although they can be successful, such control architectures have greater complexity and are more invasive for the subject wearing the device [7].

Nevertheless, there are many work related repetitive tasks where an exoskeleton could significantly reduce the physical effort of users, such as manual object manipulation on assembly lines or in logistic centers [5]. In general, motion prediction is a very ambitious goal without the use of more invasive sensing technologies, but for above mentioned repetitive tasks, prediction can be achieved using modern probabilistic trajectory representation.

Movement predictions using movement primitives: A well-established approach for trajectory representation in robotics is by encoding the trajectory using movement primitives (MPs). There are a number of different versions of MPs such as dynamic movement primitives (DMPs) [9], [10], compliant parametric dynamic movement primitives (CPDMP) [11], Gaussian Mixture Regression (GMR) [12], and probabilistic movement primitives (ProMPs) [13]. In this work, we focused on the use of ProMPs which offer a wide range of properties in one generalized framework [14]. They allow simple learning from demonstration with a low set of parameters needed to represent trajectories. Generalization to new situations is possible by specifying different end-goals or specific via-points during the execution of the trajectory as well as temporal scaling of the movement. Another important property of ProMPs is the representation of trajectories together with their variance. This allows the controllers to modulate the feedback gains based on the variance of movement and provide high precision only in certain parts of the movement, which was shown to be important for successful human-robot interaction [15], [16]. Finally, ProMPs can be successfully used to make predictions of a trajectory based on the initial samples which was successfully used for real-time prediction of human movement [17].

Exoskeleton control strategies: A viable method to provide assistance along a specified path is to use potential-field-based controllers [18], [19]. However, such control algorithms generate high forces in the event of larger errors with respect to the specified path [20]. To overcome this problem, a velocity-

field-based controller was proposed by Martinez et al. [20], which applies corrective torques based on a viscous flow field control law. They showed that this approach could effectively guide movements of the user's leg along a reference path while being less resistive to large path deviations and thus making the controller inherently safer.

In this paper we investigate whether such a velocity-field-based controller could be adapted to other applications of exoskeletons involving able-bodied humans. Additionally, we explored whether this approach could be further improved by adapting to new movements in a predictive manner. We present the use of ProMPs to generate predictions of user movement in real-time in combination with a velocity-field-based controller to provide assistance to the user for performing an arm reaching task, hereby referred to as *Predictive Assistance*. With this combination we aimed to lower the physical effort of subjects while adapting to their movements. To evaluate our approach, we performed an experimental study where we measured a set of motion-related parameters for a group of 12 participants that had to perform reaching tasks to 4 different targets with and without assistance of a haptic robot. To emphasize the importance of user movement prediction, we additionally compared the *Predictive Assistance* to a *Fixed Assistance* that does not generalize to new unknown targets.

II. METHODS

First in section II-A we describe the experimental setup, protocol and evaluation metrics used in this study. Then, in section II-B we present the methodology for generating a probabilistic model and using it to compute predictions of trajectories based on newly observed data. In II-C we present the methodology used for creating fixed reference trajectories. The predicted or fixed trajectories are the basis for generating the assistive flow field which we describe in section II-D.

A. Experimental design

Twelve healthy young adults (4 women and 8 men, age 27.1 ± 4.0 years (mean $\pm$ SD); height 176.8 ± 10.1 cm; weight 70.5 ± 13.5 kg) participated in the study. The study was carried out in accordance with the recommendations of the Slovenian National Medical Ethics Committee (No. 0120-339/2017/7) and all subjects gave written informed consent for participation.

1) Setup: Subjects sat on a chair in front of a 50 inch TV screen that was located 2 m in front of the chair. Experiments were performed using a 3 axis haptic manipulator (Haptic master Mk2, MOOG, Nieuw-Vennep, The Netherlands). The subjects were controlling the position of the cursor on screen by holding the end effector of the haptic manipulator. All reaching movements were performed in the frontal plane of the subject from left to right. Interaction force, velocity, and position of the end effector were acquired by the Haptic master with a sampling rate of 200 Hz.

The goal of the experiment was for subjects to successfully reach a target that was placed on a simulated shelf on the screen in front of them. Targets had a diameter of 4 cm and were placed in four different positions as can be seen
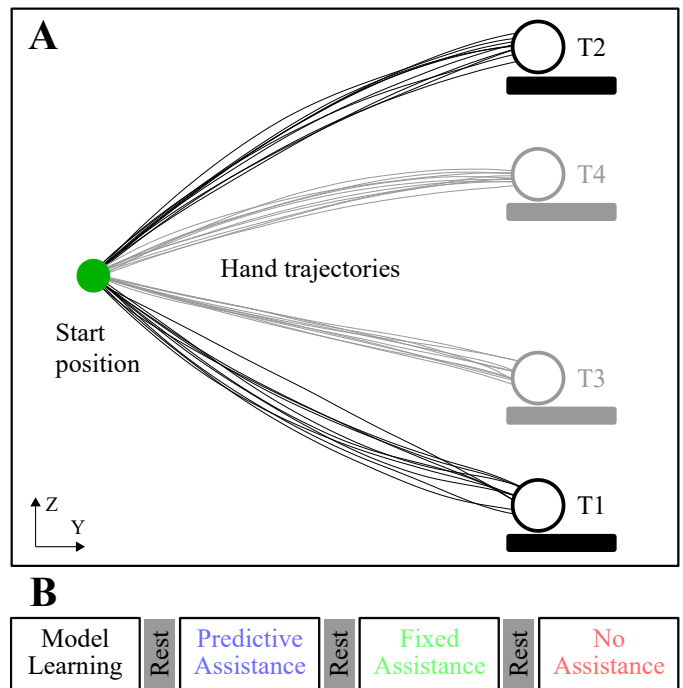

Fig. 1. Experimental setup **A**. Subjects started their movement from the start position and had to reach one of the targets positioned on the screen while avoiding the obstacles shown as black and grey rectangles. Experimental protocol **B**. Following a series of familiarization trials, subjects performed 20 trials based on which the model was learned. Each subject then performed one block of 40 trials with *Predictive Assistance*, one block with *Fixed Assistance*, and one block with *No Assistance*. The order of blocks with different conditions was randomized. There was a rest period of three minutes in between each series of trials. During the *Familiarization* and *Model Learning* phase, the task included only targets T1 and T2. In all other phases, the task consisted of reaching to all four targets.

in Fig. 1A. All the reaching movements were towards the right hand side either upward or downward. For reference, the average movement duration was 1.14 ± 0.29 s. Subjects started their movement from a circular (2.5 cm diameter) starting position in the left middle part of the screen. They were instructed to start their movement when the circle indicating the start position was coloured green and aim for the currently highlighted end target.

2) Protocol: The experiment consisted of 5 phases: *Familiarization*, *Model Learning*, *Predictive Assistance*, *Fixed assistance*, *No Assistance*. In the *Familiarization* and *Model Learning* phase, only 2 targets were part of the task (T1 and T2). The *Familiarization* phase consisted of 40 trials (20 per target) and gave the subjects time for adapting to the experimental setup. After the *Familiarization*, the *Model Learning* phase followed, which consisted of a series of 20 trials (10 per target). Only the data collected in this phase was used for generating the probabilistic model for the *Predictive Assistance* phase as well as creating the reference trajectories for the *Fixed Assistance* phase.

The condition with *Predictive Assistance* is the main focus of this study. In this condition, data collected during the *Model Learning* phase was used to make a probabilistic model with ProMPs, which was later used to make predictions in real time for new arm reaching movements. It is important to note,

that the model was trained only on targets T1 and T2, but is then tested on all 4 targets. The predicted trajectories from the ProMPs are then fed into the flow controller in order to generate the assistive forces. As a comparison, we also implemented a simple model with fixed reference trajectories that was used in the *Fixed Assistance* condition. With this we aim to emphasize the shortcoming of pre-set reference trajectories and the need of movement prediction when the task changes to new target locations (i.e. T3 and T4). Such a change is often expected in a real world scenario where we never have full a priori knowledge of the task at hand. Finally a control condition (*No Assistance*) is necessary to establish a baseline for the execution of the task. Subjects were allocated a random sequence of blocks of conditions (*Predictive Assistance*, *Fixed Assistance*, *No Assistance*) in order to mitigate the effects of fatigue on the final results. All subject performed 10 trials for each of the 4 targets (in total 40 trials per subject) in all three conditions. In between each phase of the experiment there was a rest period of three minutes. During the rest periods, subjects were given NASA TLX questionnaires [21] to mark down their perceived workload of the task in the current condition. The sequence of presented targets was randomized in all phases of the experiment. Subjects were informed whether they would receive assistance from the robot or not, but were not told about how the robot would try to assist them. The total length of the experiment was approximately 22 minutes per subject.

3) Evaluation and data analysis: To evaluate our proposed approach, we investigated the accuracy of our predicted trajectories, user effort, and potential changes in movement kinematics with metrics presented in this section.

Prediction accuracy: We analyzed the accuracy of the predicted trajectories by calculating the error of our movement predictions. We defined the error of prediction as the difference of the final point of the predicted trajectory from the centre of the target for each trial.

User effort: To estimate physical effort for performing the task, we calculated the work exerted by the subjects from the start of the movement until the target was reached. The work was calculated as the integral of force $\boldsymbol{f}_h$ over the whole path of the movement $\boldsymbol{s}$

$$W = \int \boldsymbol{f_h} d\boldsymbol{s}. \tag{1}$$

The force of the subject $\boldsymbol{f}_h$ was measured with the force sensor located at the end effector of the haptic robot. Additionally, for six subjects we also measured muscle activity. Electrodes were placed on the skin following SENIAM recommendations [22] on the anterior and posterior deltoid, biceps brachii, and triceps brachii. EMG signals were recorded at 1250 Hz. After recording, EMG signals were band-pass filtered (zero lag, 2nd order Butterworth filter with cut-off frequencies of 20 and 450 Hz), full-wave rectified and low pass filtered (zero lag, 2nd order Butterworth algorithm, 10 Hz cut-off frequency). Finally, the signal was normalized by the maximum value reached during the experiment for each subject and integrated over time (iEMG) for each trial to express the magnitude of muscle activity. From data collected with the NASA TLX questionnaires we calculated overall workload for each condition [21].

Movement kinematics: To evaluate the impact of the assistive controllers on the subjects movements, we verified how the trajectories changed in the conditions with *Predictive Assistance* and *Fixed Assistance* as compared to when subjects had no assistance in the task. First, we normalized over time all trials for each target from the condition *No Assistance* and calculated the mean of these trajectories to serve as a reference. Then, for each trial and condition, we normalized the trajectory and calculated the error from the mean reference trajectory for all data points. Finally, we calculated the root-mean-squared (rms) of this error to have a single value represent each trial.

Statistical analysis: Two-Way repeated measures ANOVAs were performed to compare the calculated parameters across the different conditions. A 4 targets (T1, T2, T3, T4) $\times$ 3 conditions (*Predictive Assistance*, *Fixed Assistance*, *No Assistance*) statistical design was used to asses the effect of the different assistive scenarios on the computed variables. Prior to analysis, the data was tested for normality (Shapiro-Wilk test) and sphericity (Mauchly's tests). Post hoc t-tests with Bonferroni correction were conducted to determine significant differences between specific conditions relative to others. For the NASA TLX score, statistical significance between *Predictive Assistance*, *Fixed Assistance* and *No Assistance* was established using a One-Way Repeated measures ANOVA and post hoc tests with Bonferroni correction.

B. ProMPs and predicted reference trajectories

1) Encoding trajectories: To reduce the amount of parameters needed to represent trajectories, ProMPs use a basis function representation approach. To better understand the formulation, we present a simple example where we describe a point in time a_t (e.g. position of the end-effector) using this method. Let $\phi_t \in \mathbf{R}^{1 \times J}$ denote a basis function vector containing values of J basis functions at time t. The variable $w \in \mathbf{R}^{J \times 1}$ represents a J-dimensional feature vector that encodes weights for each of the J basis functions. With w and ϕ_t defined, a point at time t can be approximated as

$$a_t = \phi_t \, w = \begin{bmatrix} \phi_{1,t} & \cdots & \phi_{J,t} \end{bmatrix} \begin{bmatrix} w_1 & \cdots & w_J \end{bmatrix}^T.$$

This concept can be applied to multi-dimensional states by using block diagonal matrices. Assuming that our variable a_t now has D dimensions $a_t = \begin{bmatrix} a_{1,t} & \cdots & a_{D,t} \end{bmatrix}^T$. In this case the basis function vector becomes a block diagonal matrix $\Phi_t \in \mathbf{R}^{D \times JD}$ and the weight vector w becomes a concatenation of the weight vectors of each dimension $w \in \mathbf{R}^{JD \times 1}$. Variable a_t is now approximated as

$$a_t = \Phi_t \, w = \begin{bmatrix} \phi_t & \cdots & 0 \\ \vdots & \ddots & \vdots \\ 0 & \cdots & \phi_t \end{bmatrix} \begin{bmatrix} w_1 & \cdots & w_i & \cdots & w_D \end{bmatrix}^T,$$

where

$$\phi_t = \begin{bmatrix} \phi_{1,t} & \phi_{2,t} & \cdots & \phi_{J,t} \end{bmatrix}$$

and

$$w_i = \begin{bmatrix} w_{1,i} & w_{2,i} & \cdots & w_{J,i} \end{bmatrix}^T.$$

Using the same idea we can approximate a sequence of T states denoted by $\tau = y_{1:T}$, where

$$\tau = \Phi_{1:T}w \qquad (2)$$

with

$$\Phi_{1:T} = \begin{bmatrix} \Phi_1 & \cdots & \Phi_t & \cdots & \Phi_T \end{bmatrix}^T \in \mathbf{R}^{TD \times JD},$$

where the vector w and the matrix Φ_t are the same as before. In this work we used Gaussian basis functions which are often used for point to point movements.

To approximate the trajectories in the previously described manner, the weights for each trajectory need to be calculated. For the i-th trajectory τ_i, the corresponding weight vector w_i can be estimated using a simple least squares estimate. In our case, we used the ordinary least square (OLS) method

$$w_i = \left(\Phi_{1:T}^T \Phi_{1:T} + \lambda I\right)^{-1} \Phi_{1:t}^T \tau_i, \qquad (3)$$

where λ represents a regularization parameter used to avoid numerical singularities. Its value should be small, in our case we used $\lambda = 10^{-2}$.

2) Creating the probabilistic model: When the weight vectors of all trajectories are calculated, we assume their values to be normally distributed, *i.e.*, $p(w) = \mathcal{N}(w|\mu_w, \Sigma_w)$. The mean μ_w and the covariance matrix Σ_w can be estimated with sample mean and sample covariance of the w_i vectors.

With the function approximation (2) and the weight vectors w_i defined, we can define a probabilistic model for trajectories as

$$p(\tau|w) = \prod_{t=1}^{T} \mathcal{N}(y_t|\Phi_t w, \Sigma_y) = \mathcal{N}(y_{1:t}|\Phi_{1:T}w, \Sigma_y).$$

This model describes the probability of observing a trajectory τ given the weight vector w, that is given as a linear basis function $y_{1:t} = \Phi_{1:T}w + \epsilon_{y,1:T}$. The parameter Σ_y represents independent and identically distributed (*i.i.d.*) Gaussian noise in the trajectories $y_t = \Phi_t w + \epsilon_y$, where $\epsilon_y \sim \mathcal{N}(\epsilon_y|0, \Sigma_y)$.

3) Computing Predictions from Observations: We can model predictions from observations by computing the conditional probability. First, we need to define the probability distribution over the trajectories τ, which can be computed by marginalizing out the weight vector w. In the case of a Gaussian distribution the marginal can be computed in closed form as

$$p(\tau) = \int p(\tau|w)p(w)dw$$

$$= \int \mathcal{N}(y_{1:T}|\Phi_{1:T}w, \Sigma_y)\mathcal{N}(w|\mu_w, \Sigma_w)dw$$

$$= \mathcal{N}(y_{1:t}|\Phi_{1:T}w, \Phi_{1:T}\Sigma_w \Phi_{1:T}^T + \Sigma_y). \qquad (4)$$

What we get is a multivariate Gaussian distribution, the conditional probability of which we can compute in closed form.

When we receive a previously unseen point a^*, we can predict the most likely path of the end-effector (parametrized through $\overline{\mu^*}$ and $\overline{\Sigma^*}$) by conditioning the observed state over the weight vectors. Say that we observed a sequence of states y_{t1} to y_{tM} at m=1, 2,..., M-different time points. We declare
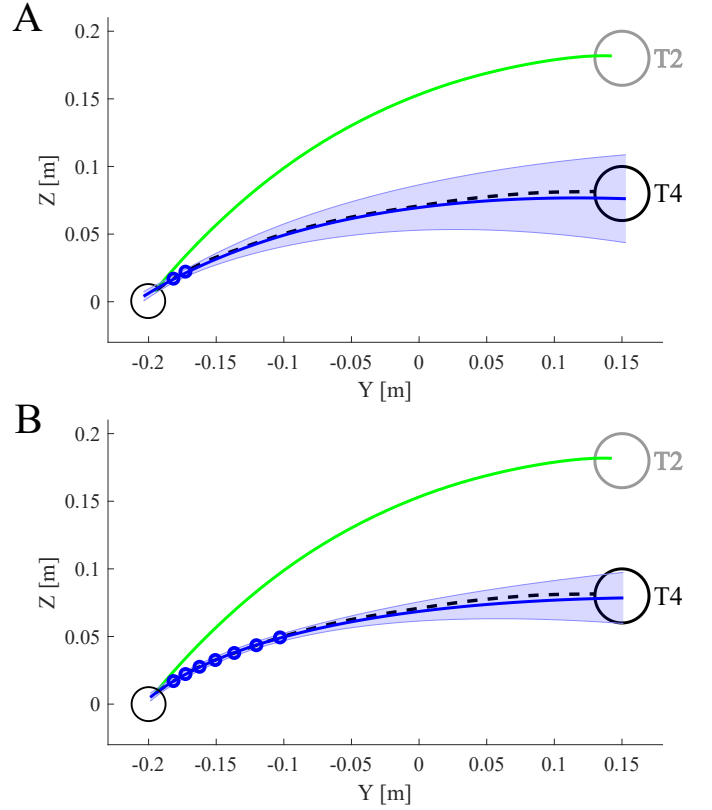

Fig. 2. Example of the fixed reference (green) and predicted reference (blue) trajectory used as the input to the flow controller for one sample trial, at two time steps. **A** 150 ms after movement onset; **B** 400 ms after movement onset. The mean and SD of the predicted trajectory is marked in blue. The black dashed line represents the actual subject movement in the condition *Predictive Assistance*.

ν as a concatenation of the observed states y_{tm} and Φ_ν as the concatenation of the basis function matrices for the observed time points.

With the observed trajectories encoded as previously described, we can obtain a conditioned distribution $p(w_\nu|\nu)$ over the weight vectors w as

$$p(w_\nu|\nu) \propto \mathcal{N}(\nu|\Phi_\nu w_\nu, \Sigma_0)p(w)$$

$$:= \mathcal{N}(w_\nu|\mu_{w|\nu}, \Sigma_{w|\nu}).$$

We can compute the mean $\mu_{w|\nu}$ and the covariance matrix $\Sigma_{w|\nu}$ as

$$\mu_{w|\nu} = \mu_w + \Sigma_w \Phi_\nu^T L(\nu - \Phi_\nu \mu_w)$$

and

$$\Sigma_{w|\nu} = \Sigma_w - \Sigma_w \Phi_\nu^T L \Phi_\nu \Sigma_w,$$

where

$$L = \left(\Sigma_0 + \Phi_\nu \Sigma_w \Phi_\nu^T\right)^{-1}.$$

With the feature mean $\mu_{w|\nu}$ and covariance matrix $\Sigma_{w|\nu}$ obtained, we can now use this conditional distribution to calculate the distribution over the trajectories $p(\overline{\tau})$ using (4)

$$p(\overline{\tau}) = \mathcal{N}(\tilde{y}_{1:T}|\Phi_{1:T}\mu_{w|\nu}, \Phi_{1:T}\Sigma_{w|\nu}\Phi_{1:T}^T + \Sigma_y),$$

where the predicted sequence of states $\tilde{y}_{1:T}$ is represented by the product $\Phi_{1:T}\mu_{w|\nu}$.

The encoding and model generation was performed based on data collected in the *Model Learning* phase of the experiment. Predictions for the subjects movement were calculated in real-time during each trial at a frequency of 20 Hz. The predictions were updating only for the first 400 ms, after which the predicted trajectory was fixed until the end of the trial. The predicted trajectories were used as a reference trajectory to generate the assistive force based on the control law specified by the flow controller. An example of the progression of the prediction during one trial is presented in Fig. 2 where we can observe how the variance of prediction decreases over time.

C. Fixed reference trajectories

To emphasize the importance of human movement prediction, we used a fixed reference assistance as a comparison. The naming "fixed" refers to the fact that this assistance does not adapt to new targets. In this case, we calculated the mean of the trajectories for each target during learning phase (T1 and T2). During the *Fixed Assistance* trial we continuously checked which of these 2 trajectories is closer to the current end effector position. The closest trajectory was selected as the reference trajectory that was passed trough to the flow controller. An example is presented in Fig. 2 where the goal was to reach target T4. In this case, the fixed reference trajectory towards T2 is closer and is the one selected as the input for the flow controller.

D. Integration with the flow controller

The velocity-field-based controller as presented in [20], shortly referred to as flow controller, generates a flow field shaped according to a reference path. In our case, the reference path used to generate this flow field was either a predicted reference trajectory or a fixed reference trajectory. We will now present the generation of the assistive flow field based on a reference trajectory.

For any given point in time, one point on the reference trajectory, denoted as x_c, will be closest to the current end effector position x. We can now define the expression for error e

$$e = x - x_c. \tag{5}$$

Additionally, we can calculate the gradient of the reference trajectory at the point x_c, to define the tangent vector t which points in the direction of the prediction. We define the normalized tangent vector as:

$$\hat{t} = \frac{t}{|t|}. \tag{6}$$

The normalized vector $\hat{n}$ is orthogonal to the tangential vector and represents the normal to the reference path at the point x_c. If we use θ to denote the angle between the error vector e and the normal to the curve $\hat{n}$, we can define a new vector $\hat{n}_i$ with the following condition:

$$\hat{n}_i = \begin{cases} -\hat{n}, & \text{if } \theta > 90 \\ \hat{n}, & \text{otherwise} \end{cases}. \tag{7}$$

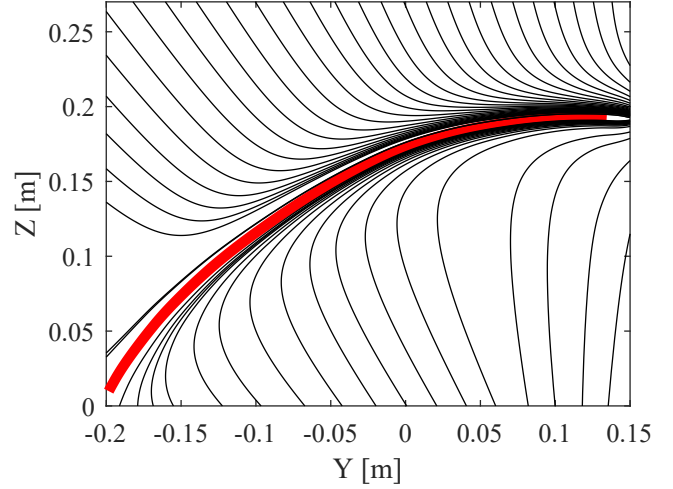This ensures that the vector $\hat{n}_i$ is always a normal vector pointing towards the reference trajectory.

Fig. 3. Example of a reference trajectory (red) with the flow field depicted as streamlines (black), $k_{sh} = 1000mm^2$. The streamlines show the shape of the flow field set by the reference velocity v_{ref}. The flow field near the trajectory is tangent (flowing in the direction of the prediction), while further away it is normal to the trajectory. With the chosen parameter k_{sh}, the vector field has a 45 degree angle with respect to the reference trajectory at a distance of $e = 3cm$. The start or the movement trajectory is located at [-0.2, 0] whereas the target is located at [0.15, 0.18].

The equation of the flow field, written as a function of error and the tangential and normal components previously defined, is given by

$$v_{ref} = \begin{cases} \Gamma(|e|\hat{n}_i + \frac{k_{sh}}{|e|}\hat{t}), & \text{for } |e| > 1e^{-5} \\ \Gamma\hat{t}, & \text{for } |e| < 1e^{-5} \end{cases}, \tag{8}$$

where the scalar Γ determines the magnitude of the velocity reference. Here $|e|\hat{n}_i + \frac{k_{sh}}{|e|}\hat{t}$ is normalized such that v_{ref} is a unit vector multiplied by Γ.

The force generated by the flow controller describes a flow force on a symmetric body due to drag when immersed in a viscous fluid:

$$F_a = C_d(v_{ref} - v). \tag{9}$$

Here C_d is equivalent to a drag coefficient and v_{ref} is the velocity of the flow field defined in Equation 8. v represents the current velocity of the point x or in our case the velocity vector of the end effector of the haptic robot. A graphical representation of the flow field v_{ref} is presented in Fig. 3. The force F_a was calculated and updated at a frequency of 200 Hz. The values of the controller parameters used in the experiment were: $\Gamma = v_{s_{max}}$, $k_{sh} = 1000$ mm^2 and $C_d = 20$ Ns/m. The magnitude of the reference velocity was calculated to match each subject's maximum velocity profile $v_{s_{max}}$ during the learning phase. This ensured that the subjects would not be forced in performing the movement faster then their preferred speed during the assisted trials. The magnitude of the reference velocity was the same for the *Predictive Assistance* and the *Fixed Assistance*. To prevent influencing the initial speed of the subject's movement, the controller was only activated 250 ms after movement onset. An example of the generated forces during one trial with *Predictive Assistance* and one trial using *Fixed Assistance* is presented in Fig. 4.
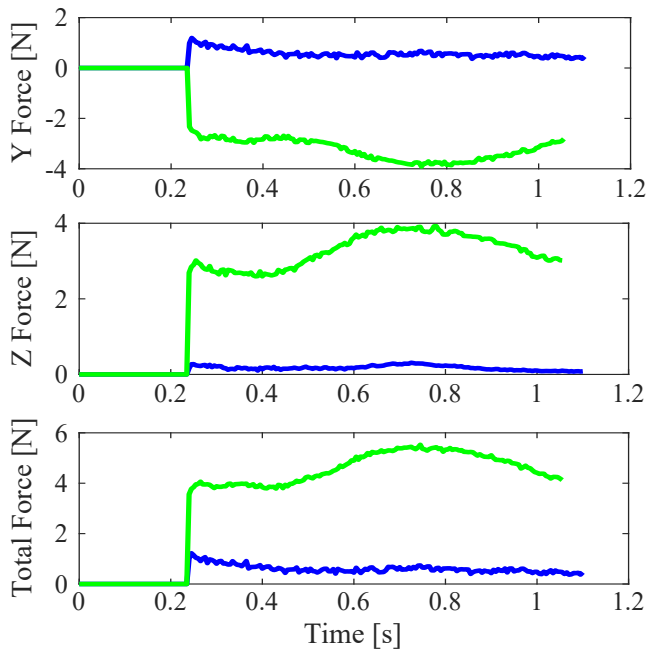
Fig. 4. Example of the commanded force during an example trial while reaching towards target T4 with assistance. **Blue** with a predicted reference trajectory, **green** with a fixed reference trajectory.
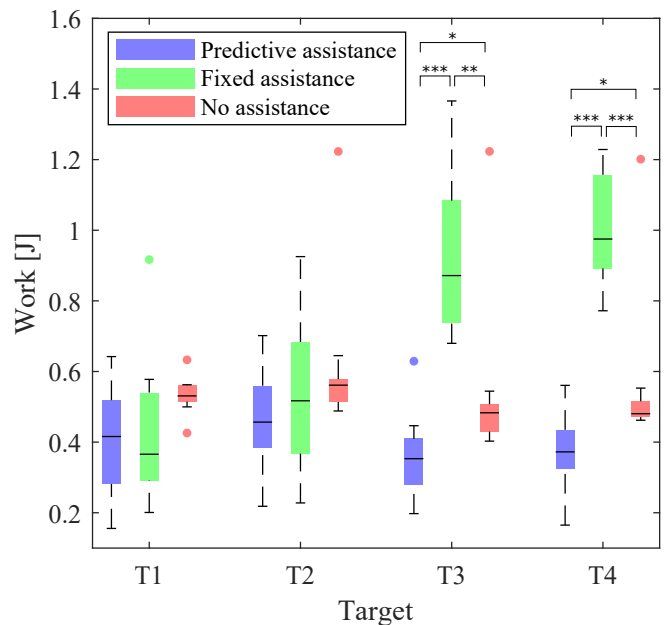

Fig. 5. Boxplots of work performed by subjects for each of the four targets and three conditions. Boxplots for the *Predictive Assistance* are highlighted in blue, for *Fixed Assistance* in green and for *No Assistance* in red. *<0.05, **<0.01, ***<0.001.

III. RESULTS

In this section we first present the accuracy of the movement predictions. We then present how the user effort was affected by analyzing the calculated exerted work, EMG muscle activity, and the NASA task load index. Finally, we present how movement kinematics are affected by the two different assistive strategies by analyzing the rms error of trajectories.

The error of the predicted trajectories was [2.3 ± 1.77 cm, 2.4 ± 1.83 cm, 2.3 ± 1.63 cm, 1.9 ± 1.24 cm] (mean $\pm$ SD) for targets T1, T2, T3, T4 respectively.

Does the predictive assistance lower user effort?: To evaluate the performance of our approach we calculated the work exerted by the subjects while performing the task. The results for each target and condition are presented in Fig. 5 in the form of boxplots. ANOVA revealed a significant main effect of controller condition on work required for task completion [$F_{(2, 22)} = 14.13$, $p = 0.001$] as well as a significant target $\times$ controller condition interaction [$F_{(6, 66)} = 65.05$, $p < 0.001$]. There was also a significant main effect of target position [$F_{(333)} = 25.28$, $p < 0.001$], which was expected since the targets are at different distances away from the starting position. For targets T1 and T2, there was no difference between the different types of assistance. However, the work required for reaching the target T3 with the *Fixed Assistance* was significantly higher compared with *No Assistance* ($t_{(11)} = 3.86$, $p = 0.008$) and *Predictive Assistance* ($t_{(11)} = 8.72$, $p < 0.001$). The same is true for target T4, where the work during *Fixed Assistance* was significantly higher compared with *No Assistance* ($t_{(11)} = 6.11$, $p = 0.002$) and *Predictive Assistance* ($t_{(11)} = 11.91$, $p < 0.001$). Additionally, we show that the work required in *Predictive Assistance* was significantly lower than in the *No*

Assistance condition at target T3 ($t_{(11)} = 2.89$, $p = 0.04$) and T4 ($t_{(11)} = 2.95$, $p = 0.04$).

As an additional measure of user effort we analyzed EMG muscle activity. For the posterior deltoid, ANOVA revealed a significant effect of condition $\times$ target interaction [$F_{(6, 30)} = 12.59$, $p < 0.001$]. Post hoc tests showed that the increase in muscle activity during *Fixed Assistance* was significantly higher compared to *No Assistance* at target T3 ($t_{(5)} = 3.82$, $p = 0.037$). For target T4 the muscle activity was significantly higher than with no assistance ($t_{(5)} = 4.79$, $p = 0.015$) and *Predictive assistance* ($t_{(5)} = 5.47$, $p = 0.008$). The results are also presented in graphical form in Fig. 6. ANOVA revealed a significant effect of condition $\times$ target interaction also for the other muscles: anterior deltoid [$F_{(6, 30)} = 2.93$, $p = 0.023$], biceps brachii [$F_{(6, 30)} = 3.26$, $p = 0.014$] and triceps brachii [$F_{(6, 30)} = 7.282$, $p < 0.001$]. However, post hoc tests did not return any significant differences between conditions at each target. The overall workload calculated from the NASA TLX questionnaires was: 18.3 ± 13.1, 41.4 ± 18.9, 21.3 ± 11.1 (mean $\pm$ SD) for the *Predictive Assistance*, *Fixed Assistance* and *No Assistance* condition respectively. ANOVA revealed a significant main effect of controller condition [$F_{(2, 22)} = 15.27$, $p < 0.001$]. Post hoc tests revealed that the workload in condition *Fixed Assistance* was significantly higher than in the condition *No Assistance* ($t_{(11)} = 4.18$, $p = 0.005$) and *Predictive assistance* ($t_{(11)} = 4.41$, $p = 0.003$). There was no significant difference between *Predictive Assistance* and *No Assistance*.

Does the predictive assistance impact the overall kinematics of the movement?: While successfully lowering the effort for performing the task is important, the assistance should not impact the overall kinematics of the movement.
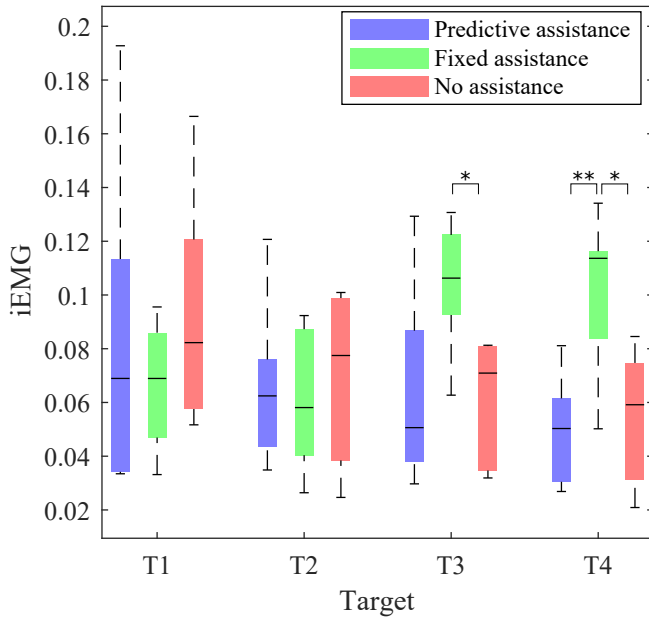
Fig. 6. Boxplots of iEMG muscle activity of the posterior deltoid for each of the four targets and three conditions. Boxplots for the *Predictive Assistance* are highlighted in blue, for *Fixed Assistance* in green, and for *No Assistance* in red. *<0.05, **<0.01, ***<0.001.
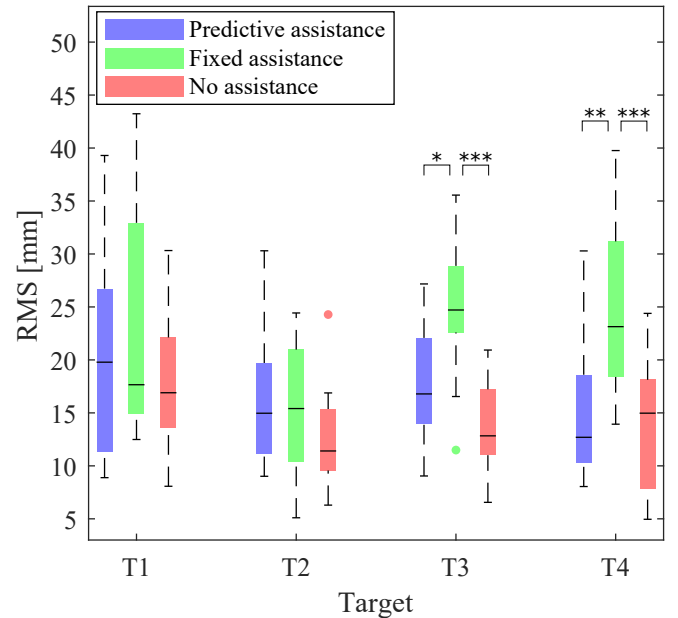
Fig. 7. Boxplots of rms deviation from a mean reference for each of the four targets and three conditions. Boxplots for the *Predictive Assistance* are highlighted in blue, for *Fixed Assistance* in green, and for *No Assistance* in red. *<0.05, **<0.01, ***<0.001.

In Fig. 7 we present the rms of the deviation from the mean trajectory calculated from the condition *No Assistance*, for each target and each condition. ANOVA revealed a significant main effect of controller condition on the rms [$F(2, 22) = 27.25$, $p < 0.001$] as well as a significant target × controller condition interaction [$F(6, 66) = 5.95$, $p < 0.001$]. There was also a significant main effect of target position [$F(3, 33) = 4.38$, $p = 0.011$]. Post hoc tests revealed, that rms values in condition *Fixed Assistance* were significantly higher than in the condition *No Assistance* at targets T3 ($t(11) = 5.20$, $p < 0.001$) and T4 ($t(11) = 5.80$, $p < 0.001$) and also significantly higher than in the condition *Predictive Assistance* for targets T3 ($t(11) = 3.06$, $p = 0.011$) and T4 ($t(11) = 4.62$, $p = 0.002$). All other comparisons were not significantly different.

IV. DISCUSSION

In this study, we investigated the efficacy of a novel exoskeleton control approach combining movement predictions with a flow field controller. Our results showed, that the probabilistic models used were able to accurately predict user movements and generalize to new target locations. This may be in part due to the fact, that the initial movement was not altered by the assistive controller and therefore the speed of movement execution was similar to those performed in the *Model Learning* phase. However, as presented in [23] it would be possible to implement a phase estimation algorithm to take into account different speeds of movement execution while maintaining reliable predictions of movements.

The analysis of work required to perform the task had expected results. Overall, the work required for completing the task was lowered using our proposed predictive control.

However, if the reference trajectory is not accurately predicted, this can still have an adverse effect on performance. This is shown by the fact that it was significantly more difficult for subjects to complete the task with the *Fixed Assistance* for targets T3 and T4. While the forces produced are not high (< 10 N) and subjects could still complete the task at hand, this had a negative effect on their performance. This was also reflected in the kinematics of the movement, the muscle activity as well as workload scores, which were all negatively affected in the *Fixed Assistance* condition.

The spread of data points for work in Fig. 5 is much lower for *No Assistance* than in the other conditions. This might indicate that the subjects started by using the same amount of work for the task, but they gradually learned how to exploit the assistance which lowered their effort for performing the task.

There was no strong indication that the *Predictive Assistance* lowered the perceived workload or muscle activity of subjects, which one might expect when considering the outcome of work analysis from the interaction force. However, this is probably because the task is not very demanding and it is therefore difficult to lower the workload even further.

V. CONCLUSION

In current exoskeleton control approaches, there exists a lack of human movement prediction without the use of invasive sensors, which is crucial for a seamless human-robot interaction. Additionally, it is very important to keep the system safe, as human safety is the single most important aspect for a successful human-robot interaction. Therefore, we proposed a novel control approach for assisting a human subject in performing a reaching task that combines movement predictions with a velocity-field-based controller.

Using ProMPs we were able to generate a model that accurately predicted user trajectories for all subsequent movements. The combination of user movement prediction with a flow controller resulted in an intuitive and safe assistance for the task. We validated our approach with an experiment emulating exoskeleton support for assisting in a reaching task, where we showed a significant reduction of effort required by the users to perform the task without affecting the user's kinematics.

For future progression of this work, we plan to further exploit the probabilistic nature of ProMPs and incorporate the predicted variance of movement in the flow controller. Meaning, we could modulate the parameter k_{sh} depending on the variance in order to provide a more restrictive flow where the movements need to be more determined whereas the flow could be more general in parts of the movement with higher variance. This would however require a different and more complex task setup with locally constrained movement trajectories (e.g. avoiding an obstacle mid trajectory) in order to properly evaluate such modulation of the flow field. Furthermore, the variance of the prediction could be used in order to determine when to "trust" the prediction more and therefore also increase the level of assistance by increasing the value of the drag coefficient C_d.

One argument could be made for using only ProMPs to generate the assistance needed for the given task, as they inherently poses properties which would probably work well in the context of our simulated task. However, even though ProMPs can provide temporal scaling of movements and lower feedback gains in parts of trajectories with high variance, we believe that a flow field controller could be inherently safer for human-robot interaction as it was argued in the work of Martinez et al. [20]. Additionally, one might argue that it would be possible to use the flow controller by itself to provide enough assistance for the task by using the average trajectories to all targets and increase the width of the flow field. However, we believe that such an approach would be too general as it would (in our case) approach a scenario with only a relatively constant force being applied in the direction of all targets.

While we showed that the proposed assistive control is capable of providing adequate assistance, future work with a direct comparison with other assistive controllers would be needed to fully evaluate this type of assistive control. Overall, we believe that our approach is a promising tool for high level exoskeleton control that can provide intuitive and safe assistance to the user for a variety of tasks.

REFERENCES

[1] T. McFarland and S. Fischer, "Considerations for Industrial Use: A Systematic Review of the Impact of Active and Passive Upper Limb Exoskeletons on Physical Exposures," *IISE Transactions on Occupational Ergonomics and Human Factors*, vol. 7, no. 3-4, pp. 322–347, oct 2019.

[2] D. Shi, W. Zhang, W. Zhang, and X. Ding, "A Review on Lower Limb Rehabilitation Exoskeleton Robots," *Chinese Journal of Mechanical Engineering (English Edition)*, vol. 32, no. 1, 2019.

[3] G. Bao, L. Pan, H. Fang, X. Wu, H. Yu, S. Cai, B. Yu, and Y. Wan, "Academic Review and Perspectives on Robotic Exoskeletons," *IEEE Transactions on Neural Systems and Rehabilitation Engineering*, vol. 27, no. 11, pp. 2294–2304, 2019.

[4] T. Proietti, V. Crocher, A. Roby-Brami, and N. Jarrasse, "Upper-Limb Robotic Exoskeletons for Neurorehabilitation: A Review on Control Strategies," *IEEE Reviews in Biomedical Engineering*, vol. 9, pp. 4–14, 2016.

[5] M. P. de Looze, T. Bosch, F. Krause, K. S. Stadler, and L. W. O'Sullivan, "Exoskeletons for industrial application and their potential effects on physical work load," *Ergonomics*, vol. 59, no. 5, pp. 671–681, 2016.

[6] M. R. Tucker, J. Olivier, A. Pagel, H. Bleuler, M. Bouri, O. Lambercy, J. d. R. Millán, R. Riener, H. Vallery, and R. Gassert, "Control strategies for active lower extremity prosthetics and orthotics: a review," *Journal of NeuroEngineering and Rehabilitation*, vol. 12, no. 1, p. 1, 2015.

[7] M. A. Gull, S. Bai, and T. Bak, "A review on design of upper limb exoskeletons," *Robotics*, vol. 9, no. 1, pp. 1–35, 2020.

[8] H. Lee, W. Kim, J. Han, and C. Han, "The technical trend of the exoskeleton robot system for human power assistance," *International Journal of Precision Engineering and Manufacturing*, vol. 13, no. 8, pp. 1491–1497, aug 2012.

[9] A. Ijspeert, J. Nakanishi, and S. Schaal, "Movement imitation with nonlinear dynamical systems in humanoid robots," in *Proceedings 2002 IEEE International Conference on Robotics and Automation (Cat. No.02CH37292)*, vol. 2. IEEE, 2002, pp. 1398–1403.

[10] A. J. Ijspeert, J. Nakanishi, H. Hoffmann, P. Pastor, and S. Schaal, "Dynamical Movement Primitives: Learning Attractor Models for Motor Behaviors," *Neural Computation*, vol. 25, no. 2, pp. 328–373, feb 2013.

[11] E. Ugur and H. Girgin, "Compliant parametric dynamic movement primitives," *Robotica*, vol. 38, no. 3, pp. 457–474, 2020.

[12] S. Calinon, D. Florent, E. L. Sauser, D. G. Caldwell, and A. G. Billard, "An approach based on Hidden Markov Model and Gaussian Mixture Regression," *IEEE Robotics and Automation Magazine*, vol. 17, no. June, pp. 44–45, 2010.

[13] A. Paraschos, G. Neumann, and J. Peters, "A probabilistic approach to robot trajectory generation," in *2013 13th IEEE-RAS International Conference on Humanoid Robots (Humanoids)*, 2013, pp. 477–483.

[14] A. Paraschos, C. Daniel, J. Peters, and G. Neumann, "Using probabilistic movement primitives in robotics," *Autonomous Robots*, vol. 42, no. 3, pp. 529–551, 2018.

[15] L. Peternel, T. Petrič, and J. Babič, "Robotic assembly solution by human-in-the-loop teaching method based on real-time stiffness modulation," *Autonomous Robots*, vol. 42, no. 1, pp. 1–17, jan 2018.

[16] L. Peternel, N. Tsagarakis, D. Caldwell, and A. Ajoudani, "Robot adaptation to human physical fatigue in human–robot co-manipulation," *Autonomous Robots*, vol. 42, no. 5, pp. 1011–1021, jun 2018.

[17] E. Rueckert, J. Čamernik, J. Peters, and J. Babič, "Probabilistic Movement Models Show that Postural Control Precedes and Predicts Volitional Motor Control," *Scientific Reports*, vol. 6, no. 1, p. 28455, sep 2016.

[18] S. K. Banala, S. H. Kim, S. K. Agrawal, and J. P. Scholz, "Robot assisted gait training with active leg exoskeleton (ALEX)," *Proceedings of the 2nd Biennial IEEE/RAS-EMBS International Conference on Biomedical Robotics and Biomechatronics, BioRob 2008*, vol. 17, no. 1, pp. 653–658, 2008.

[19] A. Duschau-Wicke, J. von Zitzewitz, A. Caprez, L. Lunenburger, and R. Riener, "Path Control: A Method for Patient-Cooperative Robot-Aided Gait Rehabilitation," *IEEE Transactions on Neural Systems and Rehabilitation Engineering*, vol. 18, no. 1, pp. 38–48, feb 2010.

[20] A. Martinez, B. Lawson, C. Durrough, and M. Goldfarb, "A Velocity-Field-Based Controller for Assisting Leg Movement during Walking with a Bilateral Hip and Knee Lower Limb Exoskeleton," *IEEE Transactions on Robotics*, vol. 35, no. 2, pp. 307–316, 2019.

[21] S. G. Hart and L. E. Staveland, "Development of NASA-TLX (Task Load Index): Results of Empirical and Theoretical Research," in *Power Technology and Engineering*, sep 1988, vol. 43, no. 5, pp. 139–183.

[22] H. J. Hermens, B. Freriks, C. Disselhorst-Klug, and G. Rau, "Development of recommendations for SEMG sensors and sensor placement procedures," *Journal of Electromyography and Kinesiology*, vol. 10, no. 5, pp. 361–374, oct 2000.

[23] G. Maeda, M. Ewerton, G. Neumann, R. Lioutikov, and J. Peters, "Phase estimation for fast action recognition and trajectory generation in human–robot collaboration," *International Journal of Robotics Research*, vol. 36, no. 13-14, pp. 1579–1594, 2017.